

Coulomb correlations and the Wigner–Mott transition

A. CAMJAYI^{1,2}, K. HAULE¹, V. DOBROSAVLJEVIĆ³ AND G. KOTLIAR^{1*}

¹Department of Physics and Astronomy, Rutgers University, Piscataway, New Jersey 08854, USA

²Departamento de Física, Comisión Nacional de Energía Atómica (CNEA), Avenida General Paz y Constituyentes, 1650 San Martín, Argentina

³Department of Physics and National High Magnetic Field Laboratory, Florida State University, Tallahassee, Florida 32310, USA

*e-mail: kotliar@physics.rutgers.edu

Published online: 26 October 2008; doi:10.1038/nphys1106

Strong correlation effects, such as a marked increase in the effective mass of the carriers of electricity, recently observed in the low-density electron gas¹ have provided spectacular support for the existence of a sharp metal–insulator transition in dilute two-dimensional electron gases². Here, we show that strong correlations, normally expected only for narrow integer-filled bands, can be effectively enhanced even far away from integer-filling, owing to incipient charge ordering driven by non-local Coulomb interactions. This general mechanism is illustrated by solving an extended Hubbard model using dynamical mean-field theory³. Our findings account for the key aspects of the experimental phase diagram, and reconcile the early viewpoints of Wigner and Mott. The interplay of short-range charge order and local correlations should result in a three-peak structure in the electron spectral function, which can be observed in tunnelling and optical spectroscopy. These experiments will discriminate between the Wigner–Mott scenario and the alternative perspective that views disorder as the main driving force for the two-dimensional metal–insulator transition⁴.

First indications of a two-dimensional metal–insulator transition (2D-MIT) have emerged from transport studies, leading to a great deal of controversy and debate². Long-held beliefs⁵ that even small amounts of impurities can destroy a Fermi liquid at zero temperature were brought into question, triggering renewed interest and activity. Careful theoretical work⁶ suggested that sufficiently strong interactions may suppress weak localization tendencies and stabilize the metal at weak disorder. More recent experiments^{1,7–11} focused on higher mobility (weaker disorder) samples, where advances in experimental capabilities enabled precision measurements of the spin susceptibility χ and the effective mass m^* . Within experimental resolution, both quantities seem to diverge at the critical density n_c , whereas the Wilson ratio $\chi/m^* = g^*$ seems to have a weaker density dependence. These findings, which have been confirmed by several complementary experimental methods^{12–14}, are most clearly pronounced in the cleanest samples, strongly suggesting that interaction effects¹—and not disorder—are the dominant driving force for the 2D-MIT¹⁵.

The divergence of the effective mass and spin susceptibility has been observed in transition-metal oxides near the density-driven Mott transition¹⁶, and in ³He monolayers near solidification¹⁷. For these materials, a description in terms of an almost localized Fermi liquid and the Brinkman–Rice theory of the Hubbard model has

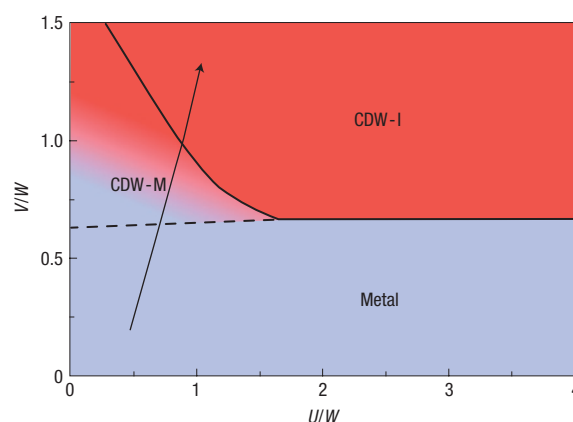


Figure 1 Phase diagram for the extended Hubbard model at quarter-filling. The on-site Coulomb interaction U and the inter-site interaction V are varied on the x and y axis, respectively. The temperature is held constant at $T = 0.01$. W is the half-bandwidth and the energy unit. A typical trajectory relevant for the 2D-MIT is shown by the arrow. The following phases are found: charge-density-wave metallic phase (CDW-M), charge-density-wave insulating phase (CDW-I).

been very successful¹⁸. The similarity between the observation in oxides, ³He and 2D electron gases (2DEGs) suggests that we should think about the physics of the 2D-MIT as yet another example of the Hubbard–Mott phenomena^{19,20}. Still, the situation relevant to the 2DEG experiments corresponds to a nearly empty conduction band—a regime very removed from near-integer-filling where Mott–Hubbard physics has been successfully applied to interpret experiments in ³He and transition-metal oxides.

Another aspect of the Hubbard–Mott picture for the 2D-MIT seems equally troubling. Early theories of the Mott transition, using the Gutzwiller variational approach¹⁸, did predict an enhanced m^* but a non-critical g^* , as seen in experiments. However, more accurate calculations using dynamical mean-field theory³ (DMFT) established that generally χ should not be expected to diverge at the transition, but should instead saturate at a finite value $\chi_c \sim 1/J$, where J is the (finite) superexchange interaction characterizing the Mott insulating phase of the lattice model in question. In this case,

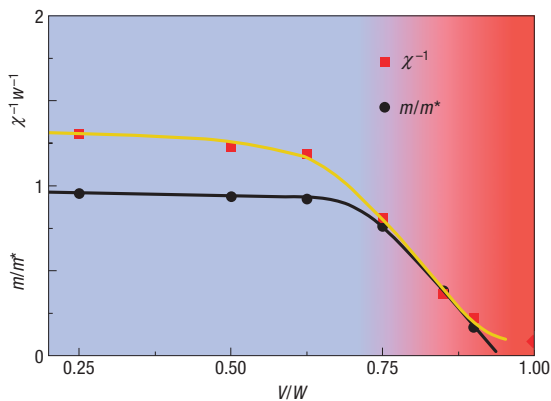


Figure 2 Inverse effective mass and spin susceptibility. These quantities are plotted along the arrow in Fig. 1. Correlation effects are markedly enhanced in the presence of charge ordering, whereas the system remains metallic. Black circles correspond to inverse effective mass m/m^* and red squares to inverse spin susceptibility χ^{-1} . The lines are guides to the eye.

g^* is expected to gradually decrease and vanish as the transition is approached—in striking contrast to the 2DEG experiments.

Should the 2D-MIT be thought of as a manifestation of Mott physics—a gradual conversion of the electrons into localized magnetic moments—or does the explanation require a completely different physical picture? Here, we provide a simple answer to this important question, and present detailed and careful model calculations to support our view. We think it is likely that near the 2D-MIT the electron gas has short-range crystalline order, which we model with a tight-binding Hamiltonian. The lattice sites represent the precursors, in the fluid phase, of vacancies and interstitials in the Wigner crystal phase. This is a lattice model at quarter-filling where the area of a cell containing two lattice sites, corresponds to an area $\pi r_s^2 a_B^2$, containing one electron in the electron gas problem. Here, r_s is the adimensional ratio between Coulomb interaction and Fermi energy, and $a_B = (4\pi\epsilon\hbar^2)/(m_b e^2)$ is the Bohr radius of the system with ϵ being the electric permittivity of the gas, \hbar the reduced Planck constant, m_b the band mass and e the electron's charge. As the system is not close to integer-filling, the non-local (inter-site) part of the Coulomb interaction cannot be neglected, as it induces significant charge correlations. These in turn enhance the role of the short-range (on-site) part of the Coulomb force, leading to strong correlation physics even far away from integer-filling. As the ratio of the Coulomb interactions to the Fermi energy increases, the system develops short-range crystalline order, which in turn allows the Hubbard interaction to be effective resulting in the signatures of Mott localization.

We neglect the effect of disorder and we focus on the extended Hubbard model²¹ as an effective Hamiltonian to describe the physics of the 2DEG at low energies. This model contains, in addition to the usual on-site Hubbard U , a nearest-neighbour inter-site repulsion V . The spirit of our approach is similar to that of the almost localized Fermi liquid framework^{18,22} that successfully described key aspects of the physics of helium near solidification.

The extended Hubbard model has been studied in detail using DMFT (ref. 3) where the non-local part of the Coulomb interaction is treated at the Hartree level. To incorporate the physics of Wigner crystallization, we consider a bipartite Bethe lattice, at quarter-filling. We have checked that all of the qualitative features discussed here do not depend on the chosen lattice. The energy is measured in units of the half-bandwidth W . U/W and V/W are then

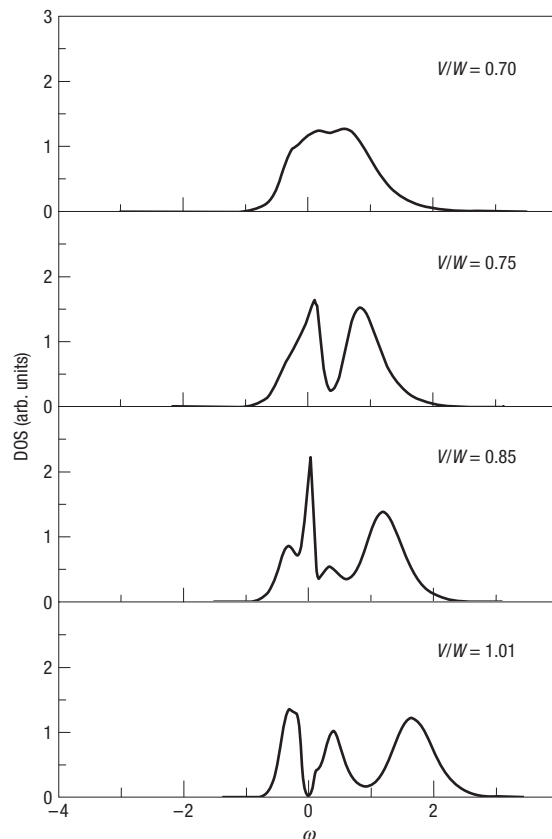


Figure 3 Evolution of the density of states. Correlations are more important as U and V increase along the path marked by the arrow in see Fig. 1, and a quasiparticle peak develops near the Fermi energy.

increasing functions of r_s , that is, decreasing functions of the electronic density, as shown by the arrow in Fig. 1. To connect the lattice model to the original electron gas model in the continuum, it is necessary to take $W = (\pi\hbar^2)/(m_b r_s^2 a_B^2)$, $V = e^2/(8\pi\epsilon a_B r_s)$ and U as an increasing function of $1/r_s$.

The self-consistent equations are:

$$G_{A,B}^{-1}(i\omega_n) = i\omega_n + \mu - 2Vn_{B,A} - \Sigma_{A,B}(i\omega_n) - G_{B,A}(i\omega_n)/4,$$

where $G_{A/B}$ are the local Green's functions, $\Sigma_{A/B}$ the self-energy, $n_{A,B}$ the occupation, μ the chemical potential and $i\omega_n$ the Matsubara's frequencies. To accurately solve the DMFT equations at low temperatures ($T = 0.01$), we use the implementation of the continuous-time quantum Monte Carlo algorithm of ref. 23.

At quarter-filling and when the inter-site interaction V vanishes, no insulating solution is found even if the interaction parameter U is arbitrarily large. For $V > 0$, charge ordering occurs. The DMFT phase diagram of the system as a function of U and V is shown in Fig. 1.

The system goes from a weakly correlated Fermi liquid (small U and V), to a charge-ordered Fermi liquid, to a Wigner–Mott insulator. It is well known that broken symmetry phases in mean-field theory are sometimes indicative of the onset of pronounced strong short-range order in the 2D system. Therefore, we cannot address with this approach the possibility of the existence of a metallic charge-ordered phase in the electron gas²⁴. The dashed line in Fig. 1 should be thought of as crossover in the 2DEG.

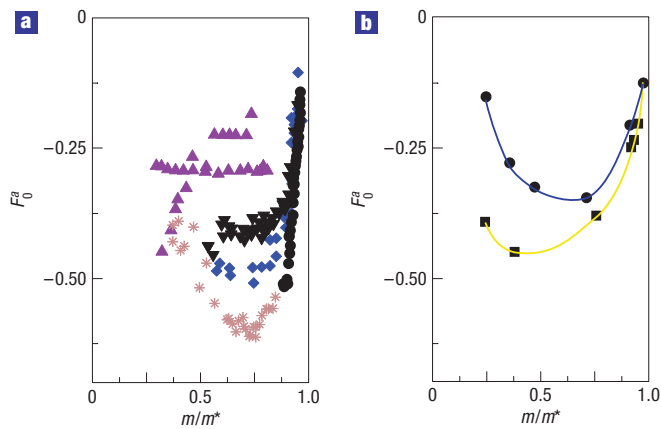


Figure 4 Behaviour of the Fermi liquid parameter F_0^a versus inverse effective mass. **a**, Experimental data showing the correlation between F_0^a and m^* . They are extracted from: ref. 8 (black circles), ref. 7 (black triangles), refs 13,25 (violet triangles), refs 26,27 (blue diamonds), ref. 28 (pink asterisks). **b**, Model calculations of the same quantity. The yellow curve corresponds to the quarter-filled case along the path marked by the arrow in Fig. 1. The blue curve shows the corresponding Mott–Hubbard results at half-filling when the on-site U is varying. The Wigner–Mott model correctly captures the experimental trend.

Remarkably strong correlation effects emerge only in the intermediate regime, where charge ordering sets in. Increasing the charge occupation on one of the two sublattices ($\langle n_A \rangle \lesssim 1$) boosts the effects of the on-site Coulomb repulsion U , and markedly increases the correlation effects. Hence, charge order leads to a marked increase of the effective mass and the spin susceptibility, whereas the system remains metallic (Fig. 2). This behaviour is strongly reminiscent of that found in the 2DEG experiments, where the mass enhancement is seen only in a narrow region preceding the metal-to-insulator transition, but not at high densities, where $m/m^* \approx 1$.

The details of the magnetic interactions very close to the 2D-MIT, as well as the different types of magnetic long-range order in the insulator, depend to some extent on the type of lattice used. Note however that the enhancement of χ at the Wigner–Mott transition, which is stronger at quarter-filling than at half-filling for the same model, is a robust feature.

In the physical picture advocated in this approach, the enhancement of the effective mass is accompanied by the development of a quasiparticle peak in the one-particle density of states, as shown in Fig. 3. The width of the quasiparticle peak is inversely proportional to m^* .

A stringent test of our scenario is the relation between the Fermi liquid parameter F_0^a ($g^* = (1 + F_0^a)^{-1}$) and the mass enhancement. Figure 4 shows the behaviour of F_0^a versus inverse mass m/m^* . The data were compiled from experiments carried out on Si-MOSFETs (refs 7,8,13,25), GaAs HIGFETs (refs 26,27) and AlAs quantum wells²⁸ using transport measurements, magnetic measurements or both. The spread between different sets of experimental data in Fig. 4a may be due to either different experimental conditions or the use of different probes for extracting the Landau parameters. Even though there is no experimentally established ‘universal trend’, the model calculations close to the Wigner–Mott transition at quarter-filling represent a clear improvement over the Mott–Hubbard picture at half-filling, capturing the qualitative behaviour of the experimental data.

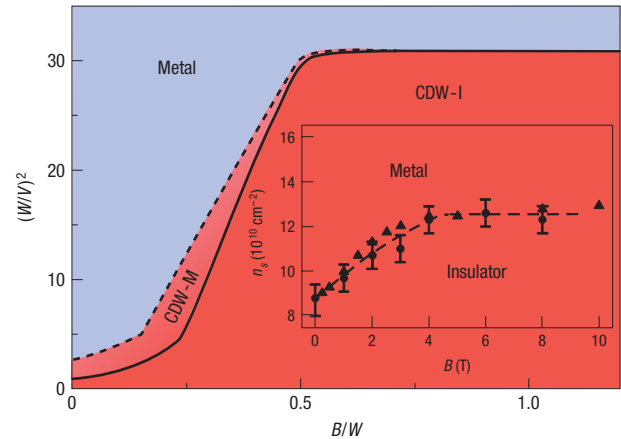


Figure 5 Magnetic phase diagram. We evolve the phases along the path in Fig. 1 by applying a parallel magnetic field. Field-driven localization is possible only sufficiently close to the Wigner–Mott transition, within the correlated regime. Inset: Experimental phase diagram. Error bars represent the standard deviation in the determination of the critical density. Adapted from refs 29 and 30.

One of the most interesting features of the 2D-MIT is the marked sensitivity of the correlated Fermi liquid regime to the Zeeman (spin) splitting introduced by applying a parallel magnetic field. Indeed, experiments demonstrated that the heavy Fermi liquid can be effectively destroyed by applying a parallel field, producing a spin-polarized insulating state above a ‘saturation field’ $B^*(n)$ of only a few teslas. For a heavy Fermi liquid, $B^* \sim 1/m^*$ is expected, and indeed experiments and our theory (see Fig. 5) show that $B^*(n) \sim (n - n_c)$, consistent with a singularly enhanced m^* at the transition. Such field-induced localization is found only in the correlated regime close enough to the transition.

This behaviour is very hard to understand from the point of view of a half-filled Hubbard model, because in this case sufficiently strong field always leads to insulating behaviour. The field response we find at quarter-filling is markedly different, as shown in Fig. 5. A field-driven localization transition is still found, but in contrast to the half-filled case, it is restricted to the strongly correlated charge-ordered region; the featureless Fermi liquid remains metallic even on spin polarization. These findings find favourable agreement with the experimentally established phase diagram (Fig. 5, inset).

The dependence of the effective mass on the applied magnetic field is relatively weak, owing to the presence of two competing effects. On one hand, the magnetic field locks the spin fluctuations, hence reducing the entropy and the effective mass of the system. On the other hand, the magnetic field enhances the charge ordering, which in turn produces a charge-density-wave (CDW) coherence peak at the band edge, enhancing the density of states.

The current theory considers the on-site Coulomb repulsion at the single-site DMFT level and the nearest-neighbour repulsion at the Hartree level. A better treatment, which incorporates dynamical charge fluctuations, the long-range Coulomb interactions and short-range correlation effects, is possible using extensions of DMFT. Furthermore, disorder effects in the strongly correlated regime need to be addressed. Although these directions remain interesting avenues for the future, we believe that the essential new physics at the Wigner–Mott transition is already captured within the present calculation.

Received 22 February 2008; accepted 10 September 2008; published 26 October 2008.

References

1. Kravchenko, S. V. & Sarachik, M. P. Metal–insulator transition in two-dimensional electron systems. *Rep. Prog. Phys.* **67**, 1–44 (2004).
2. Abrahams, E., Kravchenko, S. V. & Sarachik, M. P. Colloquium: Metallic behavior and related phenomena in two dimensions. *Rev. Mod. Phys.* **73**, 251–266 (2001).
3. Georges, A., Kotliar, G., Krauth, W. & Rozenberg, M. J. Dynamical mean-field theory of strongly correlated fermion systems and the limit of infinite dimensions. *Rev. Mod. Phys.* **68**, 13–125 (1996).
4. Punnoose, A. & Finkelstein, A. M. Metal–insulator transition in disordered two-dimensional electron systems. *Science* **310**, 289–291 (2005).
5. Abrahams, E., Anderson, P. W., Licciardello, D. C. & Ramakrishnan, T. V. Scaling theory of localization: Absence of quantum diffusion in two dimensions. *Phys. Rev. Lett.* **42**, 673–676 (1979).
6. Punnoose, A. & Finkelstein, A. M. Dilute electron gas near the metal–insulator transition: Role of valleys in silicon inversion layers. *Phys. Rev. Lett.* **88**, 016802 (2002).
7. Pudalov, V. M. *et al.* Low-density spin susceptibility and effective mass of mobile electrons in Si inversion layers. *Phys. Rev. Lett.* **88**, 196404 (2002).
8. Pudalov, V. M. *et al.* Interaction effects in conductivity of Si inversion layers at intermediate temperatures. *Phys. Rev. Lett.* **91**, 126403 (2003).
9. Zhu, J., Stormer, H. L., Pfeiffer, L. N., Baldwin, K. W. & West, K. W. Spin susceptibility of an ultra-low-density two-dimensional electron system. *Phys. Rev. Lett.* **90**, 056805 (2003).
10. Gunawan, O. *et al.* Valley susceptibility of an interacting two-dimensional electron system. *Phys. Rev. Lett.* **97**, 186404 (2006).
11. Gao, X. P. A. *et al.* Spin-polarization-induced tenfold magnetoresistivity of highly metallic two-dimensional holes in a narrow GaAs quantum well. *Phys. Rev. B* **73**, 241315 (2006).
12. Prus, O., Yaish, Y., Reznikov, M., Sivan, U. & Pudalov, V. Thermodynamic spin magnetization of strongly correlated two-dimensional electrons in a silicon inversion layer. *Phys. Rev. B* **67**, 205407 (2003).
13. Anissimova, S. *et al.* Magnetization of a strongly interacting two-dimensional electron system in perpendicular magnetic fields. *Phys. Rev. Lett.* **96**, 046409 (2006).
14. Shashkin, A. A. *et al.* Pauli spin susceptibility of a strongly correlated two-dimensional electron liquid. *Phys. Rev. Lett.* **96**, 036403 (2006).
15. Pankov, S. & Dobrosavljević, V. Self-doping instability of the Wigner–Mott insulator. *Phys. Rev. B* **77**, 085104 (2008).
16. Tokura, Y. *et al.* Filling dependence of electronic properties on the verge of metal–Mott-insulator transition in $\text{Sr}_{1-x}\text{La}_x\text{TiO}_3$. *Phys. Rev. Lett.* **70**, 2126–2129 (1993).
17. Casey, A., Patel, H., Nyéki, J., Cowan, B. P. & Saunders, J. Evidence for a Mott–Hubbard transition in a two-dimensional ^3He fluid monolayer. *Phys. Rev. Lett.* **90**, 115301 (2003).
18. Vollhardt, D. Normal ^3He : An almost localized Fermi liquid. *Rev. Mod. Phys.* **56**, 99–120 (1984).
19. Spivak, B. Properties of the strongly correlated two-dimensional electron gas in Si MOSFET's. *Phys. Rev. B* **64**, 085317 (2001).
20. Dolgoplov, V. T. On effective electron mass of silicon field structures at low electron densities. *JETP Lett.* **76**, 377–379 (2002).
21. Pietig, R., Bulla, R. & Blawid, S. Reentrant charge order transition in the extended Hubbard model. *Phys. Rev. Lett.* **82**, 4046–4049 (1999).
22. Anderson, P. W. & Brinkman, W. F. in *The Helium Liquids* (eds Armitage, J. G. M. & Farqhar, I. E.) (Academic, 1975).
23. Haule, K. Quantum Monte Carlo impurity solver for cluster dynamical mean-field theory and electronic structure calculations with adjustable cluster base. *Phys. Rev. B* **75**, 155113 (2007).
24. Waintal, X. On the quantum melting of the two-dimensional Wigner crystal. *Phys. Rev. B* **73**, 075417 (2006).
25. Gold, A. & Dolgoplov, V. T. Determination of Landau's Fermi-liquid parameters in Si-MOSFET systems. *Pis'ma v ZhETF* **86**, 687–690 (2007).
26. Tan, Y.-W. *et al.* Measurements of the density-dependent many-body electron mass in two dimensional GaAs/AlGaAs heterostructures. *Phys. Rev. Lett.* **94**, 016405 (2005).
27. Tan, Y.-W. *et al.* Spin susceptibility of a two-dimensional electron system in GaAs towards the weak interaction region. *Phys. Rev. B* **73**, 045334 (2006).
28. Vakili, K., Shkolnikov, Y. P., Tutuc, E., De Poortere, E. P. & Shayegan, M. Spin susceptibility of two-dimensional electrons in narrow AlAs quantum wells. *Phys. Rev. Lett.* **92**, 226401 (2004).
29. Jaroszyński, J., Popović, D. & Klapwijk, T. M. Magnetic-field dependence of the anomalous noise behavior in a two-dimensional electron system in silicon. *Phys. Rev. Lett.* **92**, 226403 (2004).
30. Shashkin, A. A., Kravchenko, S. V. & Klapwijk, T. M. Metal–insulator transition in a 2D electron gas: Equivalence of two approaches for determining the critical point. *Phys. Rev. Lett.* **87**, 266402 (2001).

Acknowledgements

We thank M. Gershenson for fruitful discussion. A.C. and G.K. were supported by Grant NSF DMR-0806937. K.H. acknowledges support from Grant NFS DMR-0746395 and V.D. from Grant NFS DMR-0542026.

Author information

Reprints and permissions information is available online at <http://npg.nature.com/reprintsandpermissions>. Correspondence and requests for materials should be addressed to G.K.